

Mechanism of the Anionic Wittig Rearrangement. An *ab Initio* Theoretical Study

Paola Antoniotti and Glauco Tonachini*[†]

Dipartimento di Chimica Generale ed Organica Applicata, Università di Torino,
Corso Massimo D'Azeglio, 48 I-10125 Torino, Italy

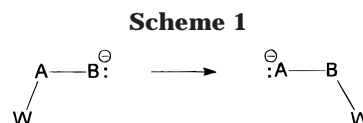
Received July 6, 1998

The mechanism of [1,2] methyl Wittig migration in the simple free and lithiated anionic H_2COCH_3 model system is investigated at the CAS-MCSCF and CCSD(T) levels of theory, providing, on one hand, a picture of the processes taking place in the gas phase and, on the other hand, two extreme descriptions of ionic association relevant to the condensed phase (absent or tight anion–cation interaction). (A) The bonding situation of the *free carbanion* correlates with the homolytic dissociation limit, but the heterolytic case is significantly lower in energy, and an avoided crossing takes place: dissociation becomes consequently heterolytic in character. However, the heterolytic limit is not necessarily attained, because nucleophilic attack on the carbonyl carbon by methide occurs before an oxygen–carbon distance of 3 Å is reached. (B) In contrast, in the *lithiated system*, the O–C bond is homolytically cleaved, because the lithium counterion stays firmly bound to oxygen, thus stabilizing the incipient radical anion of formaldehyde, and is unable to assist the O–C bond cleavage by setting an interaction with the detaching methyl carbon. The electrostatic complex between formaldehyde and methyllithium, although rather stable, does not appear to be immediately reachable, even if methyl radical can reassociate to formaldehyde radical anion not only from the same face from which it detached but also from the opposite face, attained by pivoting rather closely around lithium. The lithiated oxyanion is then readily obtained, in a radical coupling reassociation step. How solvation could modulate the cation–anion interaction is explored by allowing lithium to interact with three dimethyl ether molecules. Also this model confirms the preference for O–C homolytic cleavage. In summary, the study of this simple system clearly suggests a *mechanistic dichotomy*: the preferred heterolytic mechanism of the gas-phase reaction contrasts the homolytic cleavage indicated for the condensed phase reaction (although some dependence of the mechanism on the degree of cation–anion interaction and substitution is to be expected).

Introduction

Electrophilic rearrangements (although less common than the nucleophilic) form a vast class of reactions in which a group W migrates on an underlying skeleton A–B (*formally* without the W–A bond electrons) to bind to an electron-rich site B (Scheme 1).^{1,2} Among these, the possibly competing Stevens and Sommelet reactions,³ and the Wittig migration,⁴ can be mentioned as well-known formal examples of electrophilic rearrangements in organic chemistry.

However, it is obviously important to go beyond the formal description of the mechanism, in an effort aimed



to elucidate the true nature of the process under way. This can be done in experimental studies, by exploiting several different techniques, and can also be attempted, in a complementary way, through theoretical studies, by exploring the possible reaction pathways. Both approaches can give valuable contributions to the understanding of a reaction mechanism; however, they share a common limitation, in that they most often bring interesting pieces of evidence in favor or against some standing hypothesis but cannot commonly be general and conclusive.

The Wittig rearrangement, in particular, forms the subject of the present theoretical study. It is the transformation of an ether into its isomeric alcohol, taking place in the presence of strong bases. Commonly, in this reaction an alkyl, allyl, or aryl W group migrates from an oxygen atom to a (negative) carbon atom (Scheme 2).

Such a migration is neither limited to carbon-centered W groups nor to a carbon–oxygen skeleton. Wright and West studied the analogous anionic rearrangements of different silyl and germyl groups on carbon–oxygen or carbon–sulfur skeletons (taking place again in the presence of excess strong base),^{5a} and West reported on similar rearrangements on carbon–nitrogen or nitrogen–nitrogen skeletons.^{5b} This migration results in the trans-

[†] Fax: 39-011-6707642. E-mail: glauco@a500.ch.unito.it.

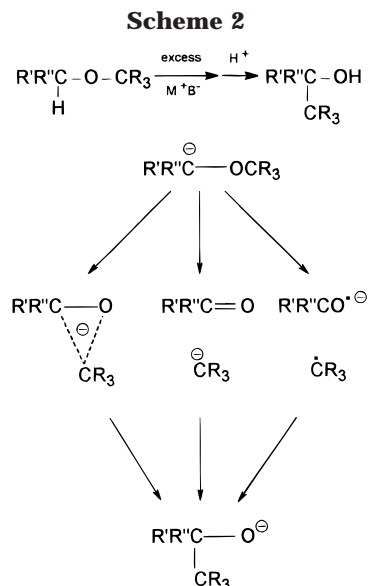
(1) See for instance: March, J. *Advanced Organic Chemistry. Reactions, Mechanisms, and Structure*, 4th ed.; J. Wiley & Sons: New York, 1992; pp 1051, 1067, 1072 and the references reported therein. For a recent theoretical study on anionic migrations, related to the present one, see: Borosky, G. L. *J. Org. Chem.* **1998**, *63*, 3337–3345.

(2) Schöllkopf, U. *Angew. Chem., Int. Ed. Engl.* **1970**, *9*, 763–773.

(3) Stevens, T. S. *Prog. Org. Chem.* **1968**, *7*, 48–74. See also ref 1, pp 673, 674, and 1100–1103 and references therein.

(4) Wittig, G.; Lohmann, L. *Ann.* **1942**, *550*, 260–268. Wittig, G. *Angew. Chem.* **1954**, *66*, 10–17. For a recent review, see: Tomooka, K.; Yamamoto, H.; Nakai, T. *Liebigs Ann./Recueil* **1997**, 1275–1281, and references therein.

(5) (a) Wright, A.; West, R. *J. Am. Chem. Soc.* **1974**, *96*, 3214–3221; 3222–3227; 3227–3232. (b) West, R. *Adv. Organomet. Chem.* **1977**, *16*, 1–30 (particularly section VII). (c) See for instance: Carey, F. A.; Sundberg, R. J. *Advanced Organic Chemistry, Part B*, Plenum Press: New York and London, 1990; Chapter 6, pp 331, 332. Wu, Y.-D.; Houk, K. N.; Marshall, J. A. *J. Org. Chem.* **1990**, *55*, 1421–1423. Mikami, K.; Uchida, T.; Hirano, T.; Wu, Y.-D.; Houk, K. N. *Tetrahedron* **1994**, *50*, 5917–5926. (d) Kawachi, A.; Doi, N.; Tamao, K. *J. Am. Chem. Soc.* **1997**, *119*, 233–234.



formation of a silyl or germyl ether (or sulfide) into its isomeric alcohol (or thiol). Recently, sila-Wittig reactions too, in which there is a [2,3] rearrangement^{5c} of an allylic group on a carbon–silicon skeleton, have been reported.^{5d} When the base is present only in catalytic amounts, the reverse migration (whose mechanism must be closely related) takes place, which is called anti-Wittig or Brook rearrangement.⁶

The rearrangements belonging to this class are formally very similar and could in principle take place with the same mechanism.⁷ In fact, a variety of mechanisms could instead operate in the different reactions mentioned above, ranging from a dissociative–reassociative process, to a two-step nondissociative mechanism (passing through a rather stable reaction intermediate), or even to a concerted mechanism (with some degree of asynchronicity). This last mechanism is formally “forbidden”,⁸ although it was suggested years ago by Dewar and Ramsden, in a study of the Stevens migration,² that Woodward–Hoffmann rules could break down for very exothermic reactions.⁹ This possible diversity was illustrated by some theoretical studies carried out in this laboratory on simple $\text{H}_2\text{CO}-\text{XH}_3$ model anionic systems, by exploring the behavior of groups centered on carbon, silicon, and germanium, migrating on the same carbon–oxygen skeleton. The first mechanistic case was exemplified by the $\text{X} = \text{C}$ choice:¹⁰ in this case, when the competition of the direct [1,2] shift (Scheme 2, left) with a dissociative process was considered in the anionic system, the former resulted not to be a realistic pathway from the carbanionic “reactant” to the oxyanionic “product”. The second

mechanism was found for $\text{X} = \text{Si}$:^{10,11} in contrast with carbon, a nondissociative migration involving a penta-coordinated-silicon cyclic intermediate was shown to be the preferred reaction pathway, either in the presence or in the absence of a lithium counterion. The last case, $\text{X} = \text{Ge}$,¹² depicted a one-step mechanism, with a significant asynchronicity in the cleavage of the O–Ge bond and formation of the new Ge–C bond.

For the Wittig rearrangement in particular, the heterolytic dissociative mechanism appeared, on the basis of the gas-phase calculations of ref 10, to be the only viable pathway. This picture (although only indirectly comparable to the experimental data in solution) impinges to some extent upon the commonly accepted mechanism of this reaction.⁷ In fact, the experiment indicates a dissociation–reassociation process (taking place in a solvent cage), but the migratory aptitudes suggest the formation of a radical pair through homolytic dissociation (Scheme 2, right) and not heterolytic cleavage of the O–C bond (Scheme 2, center). This contrast suggests to reexamine the computational results previously collected and to reinvestigate the dissociation process of the anionic system at a multideterminantal level of theory, both in the absence and in the presence of a lithium counterion. The former set of data will be directly comparable with some gas-phase results published in recent years.¹³ On the other hand, both sets of results, refined by taking into account the effect of a first solvation shell in an approximate way (see Method section), will be comparable again with the experimental evidence collected from solution chemistry. This study will therefore hopefully provide a more reliable and complete contribution to the description of the evolution of the anionic $\text{H}_2\text{CO}-\text{CH}_3$ model system; it will also allow the discussion of the possible role of the counterion and the surrounding solvent molecules in affecting the reaction mechanism. Investigations on more complex systems are under way and will form the subject of a follow-up paper.

Method

The study of the rearrangement reaction was performed by determining the critical points on the energy hypersurface corresponding to stable and transition structures. This was accomplished by way of complete gradient optimization¹⁴ of the geometrical parameters at the CAS-MCSCF level of theory,¹⁵ using the polarized split-valence shell 6-31G(d) basis sets.¹⁶ In these computations, the active space chosen consists

(11) Antonietti, P.; Canepa, C.; Tonachini, G. *J. Org. Chem.* **1994**, *59*, 3952–3959.

(12) Antonietti, P.; Canepa, C.; Tonachini, G. *Trends Org. Chem.* **1995**, *5*, 189–201. Antonietti, P.; Tonachini, G. *Organometallics* **1996**, *15*, 1307–1314.

(13) Eichinger, P. C. H.; Bowie, J. H. *J. Chem. Soc., Perkin Trans. 2* **1990**, 1763–1768. Eichinger, P. C. H.; Bowie, J. H. *J. Chem. Soc., Perkin Trans. 2* **1988**, 497–506. Eichinger, P. C. H.; Bowie, J. H. *J. Chem. Soc., Perkin Trans. 2* **1987**, 1499–1502. Eichinger, P. C. H.; Bowie, J. H.; Blumenthal, T. *J. Org. Chem.* **1986**, *51*, 5078–5082.

(14) Schlegel, H. B. In *Computational Theoretical Organic Chemistry*; Csizsma, I. G., Daudel, R., Eds.; D. Reidel Publ. Co.: Dordrecht, The Netherlands, 1981; p 129. Schlegel, H. B. *J. Chem. Phys.* **1982**, *77*, 3676–3681. Schlegel, H. B.; Binkley, J. S.; Pople, J. A. *J. Chem. Phys.* **1984**, *80*, 1976–1981. Schlegel, H. B. *Comput. Chem.* **1982**, *3*, 214.

(15) Robb, M. A.; Eade, R. H. A. *NATO Adv. Study Inst. Ser.* **1981**, *C67*, 21. See also, for a discussion of the method: Roos, B. The Complete Active Space Self-Consistent Field Method and its Applications in Electronic Structure Calculations. In *Ab Initio Methods in Quantum Chemistry-II*; Lawley, K. P., Eds.; J. Wiley & Sons Ltd.: New York, 1987.

(6) Brook, A. G.; Legrow, G. E.; MacRae, D. M. *Can. J. Chem.* **1967**, *45*, 239–253. Brook, A. G.; Warner, C. M.; Limburg, W. W. *Can. J. Chem.* **1967**, *45*, 1231–1246. Brook, A. G. *Acc. Chem. Res.* **1974**, *7*, 77–84. For a rather recent experimental paper dealing with the Brook rearrangement (in which kinetic and stereochemical results are discussed) see: Reich, H. J.; Holtan, R. C.; Bolm, C. *J. Am. Chem. Soc.* **1990**, *112*, 5609–5617.

(7) Compare with: Garst, J. F.; Smith, C. D. *J. Am. Chem. Soc.* **1976**, *98*, 1526–1537.

(8) Woodward, R. B.; Hoffmann, R. *The Conservation of Orbital Symmetry*; Academic Press: New York, 1970.

(9) Dewar, M. J. S.; Ramsden, C. A. *J. Chem. Soc., Perkin Trans. 1* **1974**, 1839–1844.

(10) Antonietti, P.; Tonachini, G. *J. Org. Chem.* **1993**, *58*, 3622–3632.

Table 1. Free Anion: Total^a and Relative^b Energies of the Critical Points

structure	CCSD(T)/6-311+G(d) ^c		CAS-MCSCF/6-31G(d)	
	<i>E</i>	ΔE	<i>E</i>	ΔE
carbanion (1a)	-154.012 872	0.0	-153.375 025	0.0
dissociation TS (1b)	-153.980 910	20.1	-153.332 379	26.8
product (1c)	-154.086 073	-45.9	-153.445 498	-44.2
homolytic diss limit	-153.968 112	28.1	-153.332 196	26.9
heterolytic diss limit	-153.999 662	8.3	-153.369 555	3.4

^a Hartrees. ^b kcal mol⁻¹. ^c Computed at the CAS-MCSCF/6-31G(d) geometries of the critical points (without the frozen-core approximation).

of four orbitals populated with four electrons. The orbitals were initially defined, to make an unambiguous choice, for three separated fragments: formaldehyde, methyl, and lithium. Two active orbitals belong to the formaldehyde-like fragment, the quasi- π and quasi- π^* couple; one is a σ orbital localized on the methyl group, and one is an empty 2s orbital of Li⁺. In this respect orbital optimization defines the more appropriate admixture of lithium empty valence sp orbitals for each structure. In this space a complete CI is performed (20 configurations). The critical points were characterized at this theory level as minima or first-order saddle points, through diagonalization of the analytically calculated Hessian matrix (vibrational frequencies calculation). In the figures which display the optimized structures, interatomic distances are in angstroms, and angles in degrees (dihedral angles are reported in parentheses). The corresponding geometries were used to recompute the relative energies by coupled cluster calculations, carried out at the CCSD(T) level,¹⁷ without the "frozen core" approximation, using the 6-311+G(d) and 6-311G(d) basis sets,¹⁶ for anionic and neutral species, respectively. This approach should be adequate for treating on the same foot homolytic and heterolytic dissociations. On one hand, CAS-MCSCF, by including a large share of nondynamical (structure-dependent) correlation, is likely to provide reasonable geometries. On the other hand, CCSD(T) calculations should offer a better estimate of reaction energies, by taking into account dynamical correlation effects too.

The role of a first solvation shell in affecting the dissociation process was explored in an approximate way, as mentioned above, by carrying out another set of optimizations, in which three dimethyl ether molecules are explicitly included to saturate the coordination of Li⁺. In view of these rather engaging "supermolecule" computations, the reliability of geometry optimizations carried out without diffuse functions was preliminarily tested by reoptimizing the dissociation saddle point of the Li(H₂COCH₃) subsystem with the 6-31+G(d) basis set¹⁶ (see next section). The agreement appeared to be satisfactory. The last part of the study was then performed, for computational feasibility, by determining the optimum geom-

Table 2. Lithiated Anion: Total^a and Relative^b Energies of the Critical Points

structure	CCSD(T)/6-311G(d) ^c		CAS-MCSCF/6-31G(d)	
	<i>E</i>	ΔE	<i>E</i>	ΔE
carbanion (3a)	-161.542 443	0.0	-160.934 391	0.0
dissociation TS (3b)	-161.481 331	38.3	-160.866 685	42.5
product (3c)	-161.617 804	-47.3	-161.009 607	-47.2
complex (4)			-160.957 635	-14.6
homolytic diss limit ^d	-161.471 515	44.5	-160.897 955	22.9
heterolytic diss limit	-161.523 652	11.8	-160.917 135	10.8

^a Hartrees. ^b kcal mol⁻¹. ^c Computed at the CAS-MCSCF/6-31G(d) geometries of the critical points (without the frozen-core approximation). ^d Methyl radical plus formaldehyde associated with neutral lithium, in an almost linear arrangement ($r_{\text{CLi}} = 20.0$ Å; $r_{\text{CO}} = 1.207$ Å; $r_{\text{OLi}} = 1.958$ Å).

Table 3. Lithiated Anion Associated with Three Dimethyl Ether Molecules: Total^a and Relative^b Energies

structure	<i>E</i>	ΔE
carbanion	-621.836 872	0.0
dissociation TS (O-C = 2.0 Å)	-621.780 523	34.8
noncritical point at O-C = 2.5 Å	-621.793 774	26.4
separated fragments (10 Å)	-621.807 766	21.4

^a Hartrees, CAS-MCSCF/6-31G(d)&3-21G optimizations. ^b kcal mol⁻¹.

tries at the CAS-MCSCF level, in conjunction with a "lightened" basis set so defined: 6-31G(d) was kept on the central system, Li(H₂COCH₃), as well as on the ether oxygens surrounding lithium; the basis set was instead reduced to 3-21G on the six ether methyl groups, supposed to play essentially a steric role. This basis set combination will be referred to as 6-31G(d)&3-21G when presenting Table 3. The GAUSSIAN94 system of programs¹⁸ was used throughout, on IBM RISC/6000 computers.

Results and Discussion

This study is articulated in three phases. In a first phase, the energy profile for methyl dissociation in the initial free carbanion (Scheme 2) is defined, to establish if heterolytic dissociation is preferred over homolytic. Then the effect of the presence of a tightly interacting lithium counterion is investigated, to assess if it can have an important role in affecting the nature of the O-C bond dissociation processes. In a third step, the energetics and structural features of the dissociation processes are reinvestigated by allowing three dimethyl ether molecules to interact with the lithium counterion through their oxygen atoms.

Dissociative Process for the Free Anion. A dissociation of the reacting system in two fragments, taking place by cleavage of the O-C bond, followed by reassociation through formation of a new C-C bond, leads to the same product obtainable in principle through a direct nondissociative [1,2] migration of the methyl group, which is formally "forbidden" by Woodward-Hoffmann rules.⁸ The optimized geometries of the initial carbanion, dissociation transition structure (TS), and final oxyanion are shown in Figure 1.

Energies relative to this system are reported in Table 1, not only for the critical points **1a-c**, but also for the homo- and heterolytic dissociation limits. The more stable ion-dipole complex (not shown) corresponds to a loose association of the formaldehyde and methide fragments, in which the negative carbon interacts with a single hydrogen of H₂CO at a distance of ca. 3 Å. Although these complexes are found as well-defined minima on the energy hypersurface, they do not need to be considered

(16) Binkley, J. S.; Pople, J. A.; Hehre, W. J. *J. Am. Chem. Soc.* **1980**, *102*, 939-947. Clark, T.; Chandrasekhar, J.; Schleyer, P. v. R. *J. Comput. Chem.* **1983**, *4*, 294. Hariharan, P. C.; Pople, J. A. *Theor. Chim. Acta* **1973**, *28*, 213-222. Frisch, M. J.; Pople, J. A.; Binkley, J. S. *J. Chem. Phys.* **1984**, *80*, 3265-3269.

(17) Coester, F.; Kümmel, H. *Nucl. Phys.* **1960**, *17*, 477. Cizek, J. *J. Chem. Phys.* **1966**, *45*, 4256-4266. Paldus, J.; Cizek, J.; Shavitt, I. *Phys. Rev. A* **1972**, *5*, 50-67. Pople, J. A.; Krishnan, R.; Schlegel, H. B.; Binkley, J. S. *Int. J. Quantum Chem.* **1978**, *14*, 545-560. Bartlett, R. J.; Purvis, G. D. *Int. J. Quantum Chem.* **1978**, *14*, 561-581. Cizek, J.; Paldus, J. *Phys. Scr.* **1980**, *21*, 251-254. Bartlett, R. J. *Annu. Rev. Phys. Chem.* **1981**, *32*, 359-401. Purvis, G. D.; Bartlett, R. J. *J. Chem. Phys.* **1982**, *76*, 1910-1918. Scuseria, G. E.; Janssen, C. L.; Schaefer, H. F., III. *J. Chem. Phys.* **1988**, *89*, 7382-7387. G. E. Scuseria, Schaefer, H. F., III. *J. Chem. Phys.* **1989**, *90*, 3700-3703.

(18) Frisch, M. J.; Trucks, G. W.; Schlegel, H. B.; Gill, P. M. W.; Johnson, B. G.; Robb, M. A.; Cheeseman, J. R.; Keith, T. A.; Petersson, G. A.; Montgomery, J. A.; Raghavachari, K.; Al-Laham, M. A.; Zakrzewski, V. G.; Ortiz, J. W.; Foresman, J. B.; Cioslowski, J.; Stefanov, B. B.; Nanayakkara, A.; Challacombe, M.; Peng, C. Y.; Ayala, P. Y.; Chen, W.; Wong, M. W.; Andres, J. L.; Replogle, E. S.; Gomperts, R.; Martin, R. L.; Fox, D. J.; Binkley, J. S.; Defrees, D. J.; Baker, J.; Stewart, J. P.; Head-Gordon, M.; Gonzalez, C.; Pople, J. A. *GAUSSIAN94*; Gaussian, Inc.: Pittsburgh, PA, 1995.

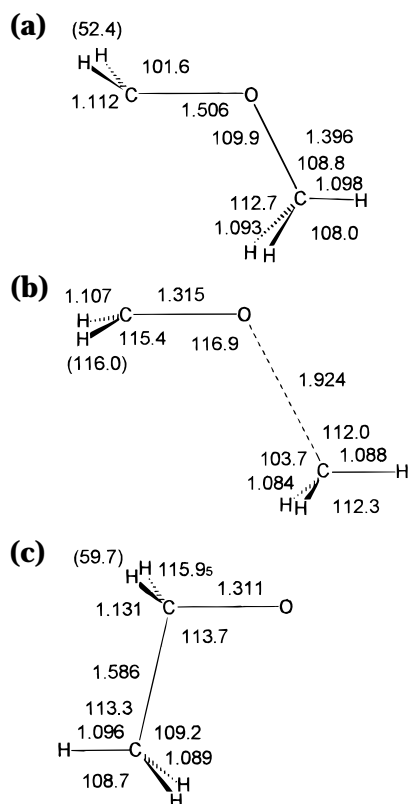


Figure 1. Free anion system: (a) the carbanionic “reagent”; (b) transition structure for methyl dissociation; (c) oxyanionic “product”. Dihedral angles are in parentheses.

as a necessary phase through which the dissociating system must pass, since the corresponding depression on the surface could as well be side-stepped by the evolving system. In the transition structure for bond dissociation **1b** the methyl moiety bears a partial negative Mulliken charge ($Q_{\text{CH}_3} = -0.191$; $Q_{\text{CH}_2} = -0.310$; $Q_{\text{O}} = -0.499$). The wave function is characterized by the dominance of one configuration (coefficient 0.957; the next contribution comes with a coefficient of -0.274). Thus the process was examined more thoroughly, by optimizing all geometrical parameters at several fixed C–O distances (R) and considering the changes in geometry and electron distribution, as well as in the nature of the polydeterminantal wave function. The results are summarized in Figure 2.

Starting from carbanion **1a**, and proceeding in order of increasing R values, the lower energy curve was obtained (Figure 2). Along this ground-state energy curve the wave function character changes rather suddenly, not in strict correspondence with the TS but at somewhat larger distances, switching from homolytic to heterolytic nature. The spin-coupling situation in **1a** would directly correlate with the homolytic dissociation limit: $\text{H}_2\text{C}-\text{O}^{\uparrow-} \downarrow\text{CH}_3$ (perfect pairing configuration) + $\lambda \text{H}_2\text{C}-\text{O}^{\uparrow-} + \text{CH}_3$ (ionic), in simple valence bond terms. But the heterolytic limit ($\text{H}_2\text{C}=\text{O} \uparrow\downarrow\text{CH}_3^-$) is lower in energy (Table 1), and symmetry allows all configurations to mix. Therefore, an avoided crossing takes place between the reactant ground state and the reactant excited state which correlates with the heterolytic dissociation limit.¹⁹ This is described in Figure 2 by the initial curve on the left (marked “homo-1”), which departs from the ground state carbanion, and

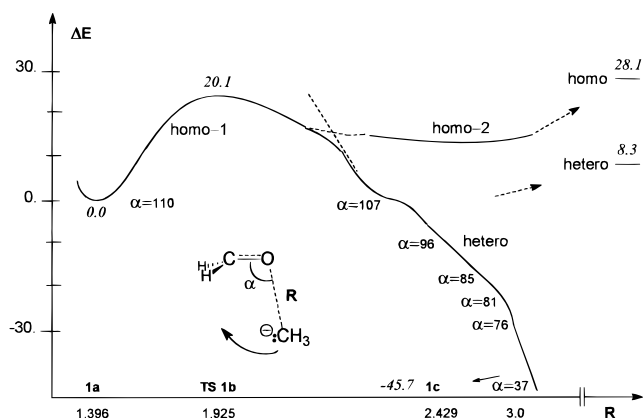


Figure 2. Free anion system: curve crossing in correspondence of methyl dissociation (see text). The picture displays the CAS-MCSCF results, while the energy difference values reported (italic, kcal mol⁻¹) are obtained at the CCSD(T)/6-311+G(d) level. The two branches labeled “homo-1” and “homo-2” correspond to the homolytic nature of the wave function; the descending branch labeled “hetero” corresponds to a methyl group charge close to 0.9.

by the upper curve on the right (marked “homo-2” in Figure 2), which share the same character. Curve homo-2 describes homolytic dissociation and was obtained by gradually reassociating the two fragments $\text{H}_2\text{CO}^{\uparrow-}$ and CH_3^{\uparrow} . The rightmost part of the lower curve (marked “hetero”) points approximately toward the heterolytic dissociation limit: but this is not attained, because at a C–O distance of ca. 3 Å, attraction between methide and the carbonyl carbon reveals itself through an abrupt closure of the COC angle, leading the two fragments toward the oxyanionic “product” **1c**. This is accompanied by a shortening of the R value and a very steep energy drop (the reaction is significantly exoergic).

In summary, the presence of a deep and extended “product basin” on the energy hypersurface does not allow a complete dissociation of the two moieties and efficiently intercepts methide on its way toward the heterolytic dissociation limit, at least within the static picture provided by these calculations. The mechanism in the gas phase, at least for this simple system, is thus probably heterolytic. A barrier of ca. 20 kcal mol⁻¹ is estimated at the coupled cluster level, somewhat lower than the CAS-MCSCF value; the two reaction energies are close in value and large (Table 1). Different systems could of course evolve through homolytic dissociation, provided that the two dissociation limits were positioned in the opposite order, thus preventing the intervention of the avoided crossing just described. In other words, if two $\text{R}_2\text{CO}^{\uparrow-}$ and CR_3^{\uparrow} fragments were at lower energy than the corresponding $\text{R}_2\text{C}=\text{O}$ and $:\text{CR}_3^-$ fragments, the reactant spin-coupling situation would directly correlate with the former along the homolytic dissociation pathway, while the energy curve of the heterolytic would not tend to intersect it. Moreover, it must be considered that the wave function nature switches to heterolytic well past the transition structure. This means (within the limits of the free anion model) that the actual nature of the two fragments can be dependent on the tightness of an hypothetical solvent cage, i.e., be a function of the R values allowed to the system.

Dissociative Process in the Lithiated System. During the C–O bond cleavage process, the behavior of

(19) Salem, L. *Electrons In Chemical Reactions. First Principles*; J. Wiley & Sons: New York, 1982.

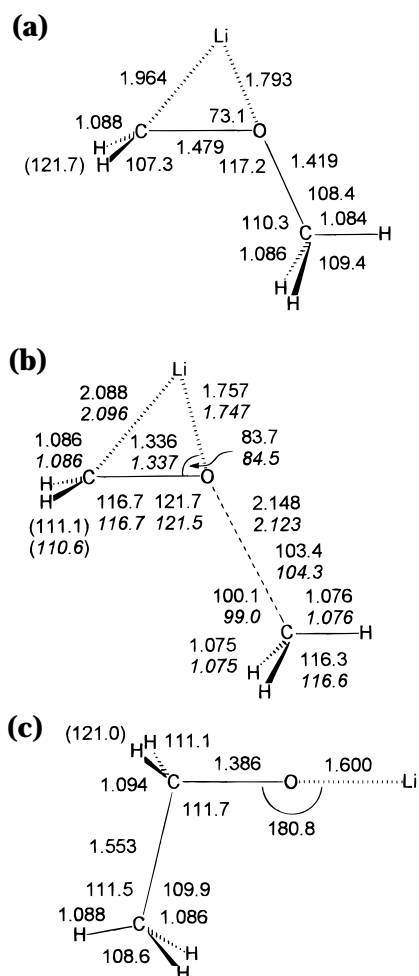


Figure 3. Lithiated anion: (a) reagent; (b) transition structure for methyl dissociation (italic numerals refer to the calculation with diffuse functions); (c) product. Dihedral angles are in parentheses.

the $(\text{H}_2\text{CO}-\text{CH}_3)\text{-Li}^+$ molecular system appears to be completely different from that just described for the free anion, mainly because lithium maintains its interaction with the H_2CO moiety in every phase of the dissociation process. This has the important consequence of stabilizing the formaldehyde radical anion/methyl radical situation against the opposite charge partitioning. Figure 3 displays the structures of the initial lithiated carbanion, transition structure for C–O bond cleavage,²⁰ and final lithiated oxyanion.

Energies and energy differences of these critical points are reported in Table 2, together with those of the separated fragments and their more stable electrostatic association, corresponding to an association of formaldehyde and lithium methide, in which lithium interacts with both the negative carbon and oxygen (Figure 4).

The energetic position of the two dissociation limits (Table 2) is qualitatively the same found for the free anion (Table 1). At the CCSD(T) level, the homolytic is significantly destabilized with respect to what was found in the free anion (Table 1), by 16.7 kcal mol⁻¹, while the heterolytic is shifted to a moderate extent, by 3.5 kcal

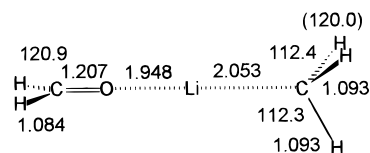


Figure 4. Electrostatic complex between formaldehyde and lithium methide. Dihedral angles are reported in parentheses.

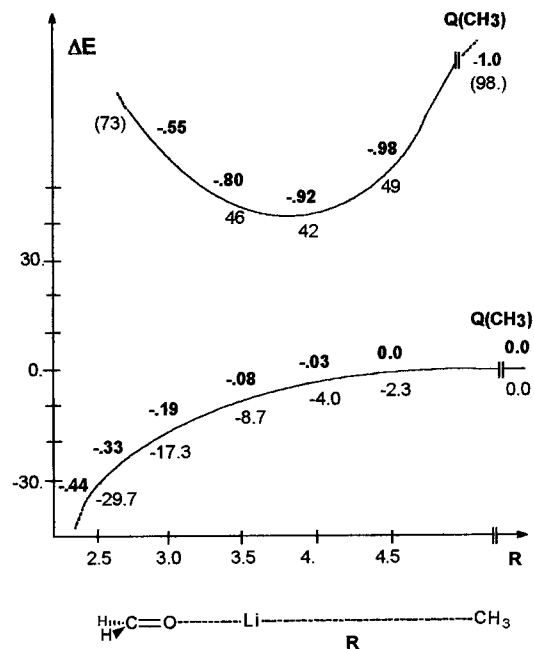
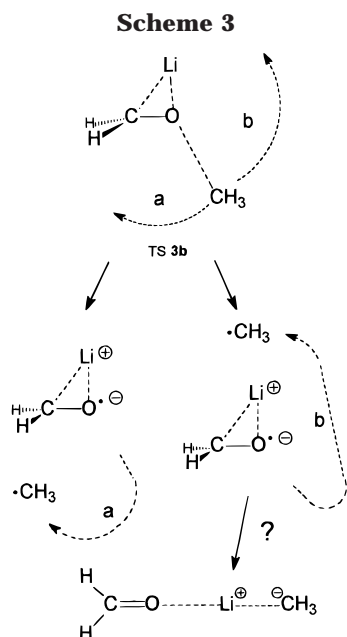


Figure 5. Formation of the electrostatic complex **4** between formaldehyde and methyl lithium, starting from the homolytic dissociation limit (formaldehyde–lithium plus methyl radical) in a quasi linear arrangement. An avoided crossing occurs, but no significant energy barrier is detected. Mulliken charges on the methyl group (bold) for the ground state and the excited state involved illustrate the change in wave function nature as Li and C approach (R). This kind of situation is never spontaneously attained.

mol⁻¹. An avoided crossing would thus occur again, if only lithium had the opportunity of exerting its stabilizing effect on an incipient methide. The lithium methide–formaldehyde complex **4** is an energy minimum endowed with remarkable stability (Table 2), from which the product **3c** could be obtained through a low-energy reassociation transition structure, similar to that found in ref 11 for the analogous silyl system (Figure 5a). However, complex **4** appears to be hardly reachable. To encourage this kind of fragmentation (heterolytic pathway), lithium should at least begin assisting the C–O bond cleavage from a bridging position right from the commencement, to subsequently privilege the interaction with a detaching methide at the expense of the initial (and strong) interaction with oxygen.

A thorough investigation of all possible geometrical changes at different stages of the dissociation process shows that, in the dissociation phase, lithium is never inclined to privilege the interaction with CH_3 at the expense of that with O (Scheme 3). In fact, it does not even attain a bridging position between O and CH_3 . Following the first dissociative phase, the CH_3 fragment can progress along two different reassociation pathways before attaining any dissociation limit. The first, geometrically more direct, possibility (Scheme 3, path a)

(20) The importance of diffuse sp functions was explored by determining structure **3b** with the 6-31G(d) and 6-31+G(d) basis sets. The geometrical parameters (Figure 3), the electron distribution, and wave function features do not show significant variations.



consists of reassociating with the H_2COLi moiety from the same face from which it detached (opposite to lithium). In this case the process is very clearly homolytic in all its phases. As an O–C distance somewhat larger than 3 Å is reached, closure of the COC angle takes place, and the product is attained.

The second reassociation pathway open to CH_3 is longer in geometrical terms but not more difficult. In fact, while moving at a rather large distance from oxygen (ca. 4 Å), methyl attains the face opposite to that from which it detached, by turning around the H_2COLi fragment (Scheme 3, path b). In doing so, the interaction of methyl carbon with lithium is significant, as witnessed by the short distances by which they are separated during the entire phase in which CH_3 swivels around the cation (ca. 2.4 Å). However, this portion of the system never becomes a methyllithium moiety (whose C–Li distance would be 2.0 Å), and Li is at all times the counterion of a negative oxygen, to which it is firmly bound. Thus, also the second pathway is unable to offer a possibility for the existence of a stabilized methide (the behavior of Li^+ in the mentioned silicon structure **5a** of ref 11 is thus quite different). Allowing, in this simple and extreme model, a lithium cation to tightly interact with the $(\text{H}_2\text{CO}-\text{CH}_3)^-$ system has the consequence of leaving homolysis as the only possibility. It has been found²¹ that the possibility of switching to the heterolytic wave function, while methyl is following pathway b, is bound to the possibility for lithium to move in the opposite direction, by opening the COLi angle. Indeed, if lithium could be about collinear to the C–O axis, then a methyl radical, located approximately on the same line at large distance, would even spontaneously collapse onto lithium, with concomitant change in wave function nature. This would occur in correspondence of an avoided crossing, as illustrated in Figure 5, but without any appreciable energy barrier (CAS-MCSCF results).

(21) To define this feature, a “fanlike” map was constructed by optimizing, for some chosen of COC and R values, all other geometrical parameters. This probed a portion of the homolytic surface (COLi = 82–89°; Li–C = 2.32–2.41 Å), as well as the heterolytic, which is below the previous one (Li–C = 2.00 Å; COLi = 156–175°). In the COLi = 110° case, the force along COLi changes sign (from negative to positive).

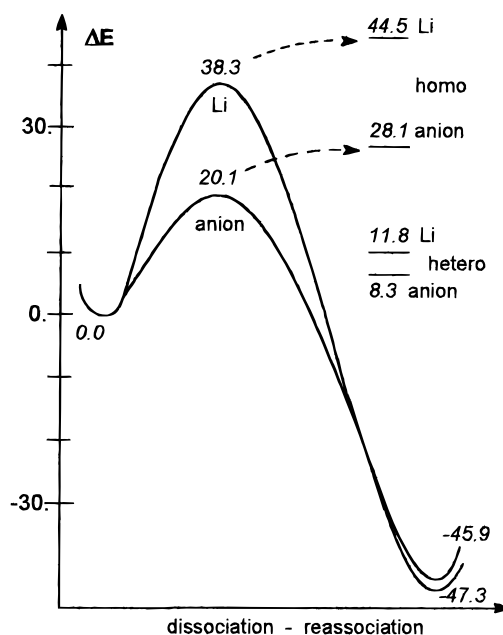


Figure 6. Comparison of the dissociation–reassociation energy profiles for the free anion system (anion) and its lithiated counterpart (Li). CCSD(T) energy differences are reported. Dashed arrows point toward the homolytic dissociation limits (homo), which are however never attained.

However, the angle COLi is a crucial parameter for wave function switching, and an energy ridge, separating this second migration pathway from a different (heterolytic) part of the hypersurface, is at the origin of the lack of Li clockwise rotation along methyl pathway b (Scheme 3).²¹

Comparison of Tables 1 and 2 shows that the dissociation process is more difficult in the lithiated system (by 18.2 kcal mol⁻¹). In contrast, the reaction energies are very close, differing only by 1.4 kcal mol⁻¹. On one hand, these data can suggest that the lithium cation stabilizes more efficiently the reactant and the product than the transition structure: this effect can be at least in part responsible of the enhanced barrier height. On the other hand, differences in ΔE^\ddagger could be related to the energetic positions of the homolytic dissociation limits, which exhibit a similar effect, being destabilized in the lithiated system by 16.4 kcal mol⁻¹ (Figure 6).

Behavior of the Lithiated System in the Presence of Dimethyl Ether Molecules. Both models discussed so far correspond to rather extreme pictures (no interaction and tight interaction with the counterion). The real situation in solution could be in between. It is however to be clearly stated that the results reported in this subsection do not have the purpose of providing *quantitative* information on solvation effects. They can rather be instrumental in attempting to assess to what degree the nature of the dissociation mechanism can be affected by solvent molecules. These molecules are allowed to interact with the counterion and can thus modulate its interaction with the anionic molecule which dissociates. In this sense, these calculations are aimed to contribute to a more realistic picture of the bond cleavage process. Thus, the computations were carried out on the “super-molecule” defined by the $(\text{H}_2\text{CO}-\text{CH}_3)^- \text{Li}^+$ system interacting with three $\text{O}(\text{CH}_3)_2$ molecules through the cation (this number saturates Li coordination without going so far as to sequester the cation). This part of

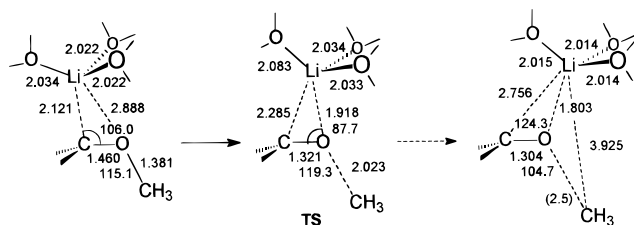


Figure 7. Reactant, transition structure for C–O bond cleavage, and additional noncritical geometry optimized corresponding to a C–O distance of 2.5 Å, just past the TS.

the study was limited for feasibility to the optimization of four points: the reactant, the transition structure for C–O bond cleavage, the separated fragments (at a C–O distance of 10 Å), and an additional noncritical geometry optimized corresponding to a C–O distance of 2.5 Å, just past the TS (Figure 7).

In the reactant a significant geometrical feature is different from that found in **3a**: the O–Li distance is 2.89 Å, testifying very little interaction, while in **3a** it was 1.79 Å. Also the C–Li distance is larger by 0.16 Å. These features obviously indicate a weakening of the cation–anion interaction operated by the three “solvent” molecules. The transition structure for methyl dissociation shows that lithium has now gained a bridging position between carbon and oxygen: however, the C–Li and O–Li distances are again larger than in **3b**, by 0.20 and 0.16 Å, respectively. As lithium leans toward pentacoordination, also the three distances with the ether oxygens stretch a little.

The electron distribution in the TS suggests homolysis, with a very modest negative charge borne by the methyl radical detaching from the H_2COLi moiety, as described by Mulliken charges: $Q_{\text{CH}_3} = -0.058$; $Q_{\text{CH}_2} = -0.025$; $Q_{\text{O}} = -0.614$; $Q_{\text{Li}} = 0.603$. These data can be compared with those of TS **3b**: $Q_{\text{CH}_3} = 0.012$; $Q_{\text{CH}_2} = 0.075$; $Q_{\text{O}} = -0.608$; $Q_{\text{Li}} = 0.521$. The extra geometry optimized at 2.5 Å (+0.5 Å with respect to the TS) has the scope of assessing how the charge distribution evolves just past the TS. Indeed, the already small negative charge of methyl tends to further decline ($Q_{\text{CH}_3} = -0.054$). The TS “earliness”, in a geometrical sense, appears to be, comparing with **1b** and **3b**, somewhat in between. Earliness can be considered in other terms, if the wave function characteristics are considered: in this sense the wave function of the present TS reflects some earliness, in that a single configuration dominates, with coefficient 0.936 (the second important configuration has a coefficient of -0.343). The slow decline of the negative methyl charge can also be attributed to this earliness. In fact, the extra point at C–O = 2.5 Å already exhibits a drop in the coefficient of the more important configuration (0.829), while the second one rises (-0.557): this is consistent with the description of a homolytic cleavage.

The energetics (available only at the CAS-MCSCF/6-31G(d)&3-21G level) are reported in Table 3. The dissociation energy barrier is lower than that associated with **3b** by 7.7 kcal mol⁻¹ (Table 2) and 8.0 kcal mol⁻¹ higher than that associated with **1b** (Table 1), thus providing an intermediate picture.

Conclusions

The mechanism of [1,2] methyl migration in the simple free and lithiated anionic methoxymethide model systems

has been discussed. This study provides, on one hand, a picture of the free anion processes which takes place in the gas phase and, on the other hand, a description of extreme and complementary situations (no anion–cation interaction or tight anion–cation interaction) conceivable as relevant to the condensed phase reaction.

The free carbanion can undergo in principle homolytic or heterolytic dissociation of the O–C bond. The “reactant” bonding situation correlates in fact with the former, but the latter is significantly lower in energy: it has been shown that an avoided crossing takes place. However, reassociation of methide to formaldehyde takes place before an oxygen–carbon distance of 3 Å is reached. Through this nucleophilic attack to the carbonyl carbon, the oxyanionic “product” is thus easily obtained. It can be however expected that substitution of the H_2C hydrogens with other groups, or detachment of a group different from methyl, could modulate the relative energetic positions of the two dissociation limits. In case they were switched, the avoided crossing itself would be removed and homolysis induced. In principle, the gas-phase mechanism could thus be variable.

When a lithium counterion is associated with the above system, the description of the O–C bond cleavage process changes significantly: the O–C bond is now homolytically cleaved, because the lithium counterion maintains its preferential interaction with oxygen and is not prone to assist the O–C bond cleavage by simultaneously engaging oxygen and the detaching methyl carbon. The electrostatic complex between formaldehyde and methyllithium has been found to be a rather stable species, yet reachable only if lithium were inclined to put itself collinear to the C–O axis by pivoting around oxygen: but lithium, although “naked”, does not tend to do so spontaneously and homolysis occurs. This outcome contrasts the heterolytic mechanism found for the gas-phase reaction. The resulting antithesis suggests some dependence of the mechanism on the degree of cation–anion interaction in the condensed phase.

The “supermolecule approach” offers a picture of a molecular system in which the coordination of the counterion is saturated, and its initial interaction with the H_2CO oxygen is weakened. The interaction between solvent molecules and Li^+ can be reckoned to affect the description of the dissociation mechanism by modulating the interaction of the counterion with the rest of the system. This part of the study confirms, however, the preference for homolytic cleavage of the O–C bond. On one hand, it indeed provides a description, which, in terms of energy differences, geometrical parameters, and charge distribution, is intermediate between the preceding ones. On the other hand, a possible interaction of Li^+ with the detaching methyl, able to trigger the transition to heterolysis, appears to be even less likely, due to the encumbrance of the ether molecules.

In conclusion, if this last situation is considered as a more realistic “extreme”, opposite to the free-anion case, the overall picture suggests a dependence of the mechanism on the degree of cation–anion interaction in the condensed phase.

Acknowledgment. Financial support has been provided by the Italian MURST and by the Italian CNR (within the Progetto Strategico “Tecnologie Chimiche Innovative”).